Виконано розрахунок розподілу щільності вихрових струмів для трьох типів котушок збудження рухомих накладних вихрострумових перетворювачів, зокрема кругової, прямокутної, ортогонально-прямокутної форм, за формулами «точних» електродинамічних математичних моделей із врахуванням ефекту швидкості.

Встановлено час розрахунку для котушки збудження кругової форми із площею зони контролю 50×50 мм при швидкості υ_x=40 м/с, який складає від 8 до 20 годин. Час розрахунку для котушки збудження прямокутної форми при швидкості по двом складовим υ_x, υ_y=20 м/с із площею зони контролю 80×48 мм складає від 8 до 9 годин. Для котушки збудження ортогонально-прямокутної форми розміром 12×12 мм час розрахунку із площею зони контролю 15×35 мм при швидкості по двом складовим υ_x, υ_y=40 м/с складає понад 7 годин; а для котушки розміром 12×24 мм при υ_x, υ_y=40 м/с – складає понад 9 годин. Виявлено, що обчислювальна складність розрахунку розподілу щільності вихрових струмів за «точними» математичними моделями при зміні навіть двох просторових координат у зоні контролю є досить великою. Тобто використовувати «точні» математичні моделі безпосередньо, розраховуючи значення розподілу щільності вихрових струмів в точках контрольованої зони, недоцільно з огляду на значну ресурсоємність обчислювального процесу.

Обґрунтовано необхідність використання для проектування вихрострумових перетворювачів з однорідним розподілом щільності вихрових струмів в зоні контролю математичного апарату сурогатної оптимізації.

Дане дослідження є корисним для спеціалістів з неруйнівного контролю в галузі машинобудування. Результати досліджень можна застосовувати для вдосконалення конструкцій вихрострумових перетворювачів з покращеними метрологічними характеристиками, зокрема однорідна чутливість, локалізація зондуючого поля збудження, підвищена завадозахищеність, можливість позбутися проявів крайового ефекту при контролі

Ключові слова: оптимальний синтез, вихрострумовий перетворювач, розподіл щільності вихрових струмів, обчислювальна ресурсоємність

UDC 620.179.147 : 519.853.6
DOI: 10.15587/1729-4061.2018.143309

STUDYING THE COMPUTATIONAL RESOURCE DEMANDS OF MATHEMATICAL MODELS FOR MOVING SURFACE EDDY CURRENT PROBES FOR SYNTHESIS PROBLEMS

R. Trembovetska
PhD, Associate Professor*
E-mail: r.trembovetska@chdtu.edu.ua
V. Halchenko
Doctor of Technical Sciences, Professor*
E-mail: halchvl@gmail.com
V. Tychkov
PhD, Associate Professor*
E-mail: v.tychkov@chdtu.edu.ua
*Department of instrumentation, mechatronics and computer technologies
Cherkasy State Technological University
Shevchenka blvd., 460, Cherkasy, Ukraine, 18006

1. Introduction

Today, the eddy current testing method and devices based on it are widely used for nondestructive testing in industry, e. g. for material discontinuity detection in defectoscopy and defectometry; measuring dimensions of testing objects (TO) and vibration parameters in thickness metering and vibrometry; definition of physical and mechanical parameters and structural state of materials in structuroscopy; detection of electric conducting objects, etc.

An important characteristic of the eddy current method is its sensitivity which depends on testing conditions, product material and positional relationship of the eddy current probe (ECP) and TO. For example, in the process of eddy current defectoscopy, sensitivity will be zero if surface crack of a finite length is located under the geometric center of the probe winding. Minimum sensitivity is observed when crack is parallel to the eddy current direction. Maximum sensitivity will be if the crack is perpendicular to the eddy current direction.

To reduce dependence of probe sensitivity to defects on ECP position relative to TO, it is necessary to ensure homogeneous distribution of the eddy current density (ECD) in the testing zone. It is technically impossible to implement such distribution in classical ECP designs. This problem can be solved by applying an optimal parametric synthesis of ECP excitation coil structure. In order to solve the optimal synthesis problem, it is necessary to solve the analysis problem over and over again for each excitation structure performing calculation of ECD for a set of points in the testing zone. Urgency of this task consists in a necessity of studying the possibility of using mathematical models of moving ECP

obtained by analytical methods (which will be called "exact" models hereinafter) as components of target functions in the problems of optimal synthesis. The studies are aimed at determining computational and time resources required for a one-time calculation of the target function in the problems of optimal synthesis of various ECP structures. In a case when requirements exceed critical values of resources, possibility of this task realization becomes problematic in general and a need for another approach significantly differing from the classical one arises, namely, application of a mathematical substitute model suitable for real calculations in the process of synthesis which will be called a metamodel. The metamodel approximates the "exact" mathematical model, that is, it is the model of model.

2. Literature review and problem statement

A linear problem of ECP synthesis with a target excitation field structure in the testing zone was solved in [1]. This problem is characterized by relative simplicity of the mathematical models used which is due to the linear dependence of the generated field on excitation current density. The drawback of linear synthesis consists in obtaining actual values of current density in the coil sections which greatly complicates practical implementation of the probes. The variant of a fixed probe is considered. The question of when the desired field structure is reached by means of the probe parameters nonlinearly included in the formula for calculation of the excitation field remains unresolved. This approach makes the ECP design much simpler.

Solution to the problem of spatial position of the excitation coil sections and determination of their geometric dimensions under the condition of fixed excitation current density, that is, the problem of nonlinear optimal synthesis, is proposed in [2]. The problem was stated as an optimization problem in which an algorithm suitable for multidimensional "ravine" target functions is used in a search for an extremum. The problem of synthesis of a fixed probe is considered. The aforementioned approaches considered in [1, 2] are designed for parametric optimization and the problem of choosing the ECP excitation system structure, that is, the number of coil sections, remains unresolved. This is caused by subjective difficulties of structure selection which can result in obtaining of its unsuccessful variant. The error in selecting the structure cannot be fixed by means of parametric optimization. The way to overcome these difficulties namely, the method of structural-parametric synthesis of the source of electromagnetic excitation field is proposed in [3]. The effect of speed is not taken into account which is a problematic unresolved part of the study.

A methodology of optimization of the excitation system design by using a planar coil of linear eddy currents was proposed in [4] for obtaining tangential and uniform distribution of eddy currents with the use of a multi-purpose genetic optimization algorithm. This approach allows one to take into account many various requirements to the probe being designed. Still unresolved is the accounting of the speed effect. Inn addition, the issue of synthesis for frame probe designs was not considered.

The method of finite elements is used in [5, 6] for synthesis in conjunction with Monte Carlo optimization methods and the genetic algorithm. The use of numerical methods for analyzing the excitation field improves accuracy of calculation on the one hand and significantly increases simulation time on the other hand. Studies were limited to planar coils of linear eddy currents and coils of a round shape. Regarding the frame ECP, no studies were conducted and the contribution of carry currents to excitation field formation was not taken into account.

An idea to suppress eddy currents on TO surface and thereby realize deeper penetration of eddy currents into material is proposed in [7]. This idea was realized by a combination of several coils fed by excitation currents with different amplitudes and phases which provides the possibility of emulation of the desired effect. Unresolved issues in this study include determination of the number of coils in the excitation system to provide the desired effect and ignoring the effect of carry currents in TO for moving ECPs.

Rotational excitation field was generated in [8] by means of a system of rotating orthogonal coils. First, an optimized distribution of ECD was calculated which provides uniform sensitivity to flaws regardless of their orientation in space and then the coil with uneven winding was designed. Distribution of coil excitation currents was optimized by the method of polynomial approximation. Complicated implementation of the excitation system which must perform rotational motion is the problematic point of the study.

The study analysis gives grounds to state that it is expedient to create systems of ECP excitation of circular and frame shapes moving over TO with a uniform distribution of electromagnetic excitation field. Such distribution ensures uniform sensitivity to defects of all spatial orientations regardless of their relative position to the ECP measuring coil. Solution to this problem consists in optimal synthesis of the ECP excitation system.

3. The aim and objectives of the study

The study objective is to evaluate, in the sense of computational cost, the possibility of calculating ECD in spatially distributed testing points on the object surface within the testing zone for the ECP synthesis problems using "exact" electrodynamic models. This will make it possible to determine resource needs of "exact" models and evaluate realizability of optimization procedures proceeding from the timetable.

To achieve this objective, the following tasks were solved:

– based on the "exact" electrodynamic mathematical models of surface ECP and using tools of the MathCAD package, create computer models for calculating the ECD distribution in the probe testing zone taking into account the speed effect;

– to carry out model calculations in order to determine timetable for their implementation;

– to evaluate the possibility of using "exact" mathematical electrodynamic models for optimal ECP synthesis.

4. Mathematical models of surface eddy current probes taking into account the speed effect

The objective function for statement of the optimal synthesis problem is as follows:

$$F_{target} = \sum_{i=1}^{N} \left(J - J_{reference} \right)^2 \rightarrow \min, \quad (1)$$

where J is the ECD distribution in the testing points on the TO generated by the excitation coil and determined

by the "exact" electrodynamic mathematical model; $J_{reference}$ is the target homogeneous ECD distribution; N is the number of testing points in the zone.

The mathematical model of ECD distribution in the testing points represents a complex functional dependence on the set of parameters, namely: spatial coordinates, elevation of the probe above TO, geometrical parameters of the excitation coil, frequency and strength of excitation current, electrophysical parameters of the material, TO speed, etc. obtained from Maxwell differential equations:

$$\nabla\times\vec{H}=\vec{J};\ \ \nabla\times\vec{E}=-\frac{d\vec{B}}{dt};\ \ \ \nabla\cdot\vec{B}=0, \tag{2}$$

taking into account $\nabla\cdot\vec{J}=0$ and the material equations

$$\vec{\mathrm{B}}=\mu_r\cdot\mu_0\cdot\vec{\mathrm{H}},\ \ \vec{\mathrm{D}}=\varepsilon\cdot\varepsilon_0\cdot\vec{\mathrm{E}},$$

where ∇ is the differential nabla operator

$$\nabla=\frac{\partial}{\partial x}\vec{\mathrm{i}}+\frac{\partial}{\partial y}\vec{\mathrm{j}}+\frac{\partial}{\partial z}\vec{\mathrm{k}};$$

$\vec{\mathrm{H}}$ – vector of magnetic field strength; $\vec{\mathrm{J}}$ – vector of current density; $\vec{\mathrm{B}}$ – vector of magnetic induction; $\vec{\mathrm{D}}$ – vector of electric induction; $\vec{\mathrm{E}}$ – vector of electric field strength; μ_r – relative magnetic permeability of the medium;

$\mu_0=4\cdot\pi\cdot10^{-7}\frac{H}{m}$ – magnetic constant in vacuum;

ε – relative electrical penetration;

$\varepsilon_0=\frac{1}{36\cdot\pi}\cdot10^{-9}\frac{F}{m}$ – electric constant in vacuum.

Since TO is movable, it is necessary to additionally take into consideration induced eddy currents, that is, the speed effect. Then, the vector of current density at $\vec{\upsilon}=(\upsilon_x,\upsilon_y,0)$ is described by the following equation which takes into account conduction and carry currents:

$$\vec{\mathrm{J}}=\sigma\cdot\left(\vec{\mathrm{E}}+\vec{\upsilon}\times\vec{\mathrm{B}}\right), \tag{3}$$

where σ is electrical conductivity.

Using formulas (2) and (3), magnetic induction $\vec{\mathrm{B}}$ in a moving conductive TO is determined from equation [9]:

$$\nabla^2\vec{\mathrm{B}}-\sigma\cdot\mu\cdot\upsilon_x\cdot\frac{\partial\vec{\mathrm{B}}}{\partial x}-\sigma\cdot\mu\cdot\upsilon_y\cdot\frac{\partial\vec{\mathrm{B}}}{\partial y}-j\cdot\omega\cdot\sigma\cdot\mu\cdot\vec{\mathrm{B}}=0, \tag{4}$$

where υ_x, υ_y are the components of the excitation coil motion speed;

$$\nabla^2B=\frac{\partial^2B}{\partial x^2}+\frac{\partial^2B}{\partial y^2}+\frac{\partial^2B}{\partial z^2}.$$

The differential equation is solved under the following assumptions and boundary conditions:

– medium is linear, homogeneous, isotropic;

– the testing object is moving, conductive, has infinite width and length and finite thickness, d;

– the coil is in one position above the object;

– the coil is excited by alternating current I with frequency ω;

– the coil conductor is infinitely thin;

– electrical conductivity, σ, magnetic permeability, μ_r and speed of motion, $\vec{\upsilon}$, are constant;

– tangential components H and normal components B on the interface between the media 1 (air) and 2 (TO medium) are continuous:

$$H_{1t}=H_{2t},\ \ B_{1n}=B_{2n}.$$

For solution of the differential equation (4) in partial derivatives, Fourier method of integral transformations in the Cartesian coordinate system is used, that is, first, direct double transformation [9–13]:

$$b(\xi,\eta,z)=\int_{-\infty}^{\infty}\int_{-\infty}^{\infty}B(x,y,z)\cdot e^{j(x\xi+y\eta)}\mathrm{d}x\mathrm{d}y, \tag{5}$$

thereby, the independent variables x and y are temporarily excluded from the equation. As a result, a common differential equation for the image is obtained:

$$\frac{\partial^2\vec{b}}{\partial z^2}-\left(\xi^2+\eta^2-j\cdot\sigma\cdot\mu\cdot\upsilon_x\cdot\xi-\right.$$
$$\left.-j\cdot\sigma\cdot\mu\cdot\upsilon_y\cdot\eta+j\cdot\omega\cdot\sigma\cdot\mu\right)\cdot\vec{b}=0. \tag{6}$$

Solution to equation (6) gives components of the magnetic flux density, b_x, b_y, b_z, that is, their form, by Fourier, for example, for the case when $d<z<0$ (Fig. 1):

$$b_x=\frac{\mu_r}{1-e^{2\cdot\gamma\cdot d}}\left[\left\{-(1+\lambda_0)\cdot e^{2\cdot\gamma\cdot d}+\nu_0\cdot e^{\left(\gamma-\sqrt{\xi^2+\eta^2}\right)d}\right\}\cdot e^{\gamma\cdot z}+\right.$$
$$\left.+\left\{1+\lambda_0-\nu_0\cdot e^{\left(\gamma-\sqrt{\xi^2+\eta^2}\right)d}\right\}\cdot e^{-\gamma\cdot z}\right]\cdot C_{ix};$$

$$b_y=\frac{\mu_r}{1-e^{2\cdot\gamma\cdot d}}\cdot\left[\left\{-(1+\lambda_0)\cdot e^{2\cdot\gamma\cdot d}+\nu_0\cdot e^{\left(\gamma-\sqrt{\xi^2+\eta^2}\right)d}\right\}\cdot e^{\gamma\cdot z}+\right.$$
$$\left.+\left\{1+\lambda_0-\nu_0\cdot e^{\left(\gamma-\sqrt{\xi^2+\eta^2}\right)d}\right\}\cdot e^{-\gamma\cdot z}\right]\cdot C_{iy};$$

$$b_z=\frac{\mu_r}{1-e^{2\cdot\gamma\cdot d}}\cdot\left[\left\{-(1+\lambda_0)\cdot e^{2\cdot\gamma\cdot d}+\nu_0\cdot e^{\left(\gamma-\sqrt{\xi^2+\eta^2}\right)d}\right\}\cdot e^{\gamma\cdot z}-\right.$$
$$\left.-\left\{1+\lambda_0-\nu_0\cdot e^{\left(\gamma-\sqrt{\xi^2+\eta^2}\right)d}\right\}\cdot e^{-\gamma\cdot z}\right]\cdot C_{iz}; \tag{7}$$

where C_{ix}, C_{iy}, C_{iz} are the coefficients taking into account the function of the probe shape;

$$C_{ix}=\frac{\mu_0\cdot I\cdot\xi}{2\cdot\eta}\cdot e^{-z_0\cdot\sqrt{\xi^2+\eta^2}}\cdot S(\xi,\eta);$$

$$C_{iy}=\frac{\mu_0\cdot I}{2}\cdot e^{-z_0\cdot\sqrt{\xi^2+\eta^2}}\cdot S(\xi,\eta);$$

$$C_{iz}=j\cdot\frac{\mu_0\cdot I\cdot\sqrt{\xi^2+\eta^2}}{2\cdot\eta}\cdot e^{-z_0\cdot\sqrt{\xi^2+\eta^2}}\cdot S(\xi,\eta);$$

$S(\xi,\eta)$ is the function of the coil shape;

$$S(\xi,\eta)=-j\cdot\frac{2\cdot\pi\cdot a\cdot\eta}{\sqrt{\xi^2+\eta^2}}\cdot J_1\left(a\cdot\sqrt{\xi^2+\eta^2}\right) \text{ for Fig 1, } a;$$

$$S(\xi,\eta)=-j\cdot\frac{4}{\xi}\cdot\sin(a\cdot\xi)\cdot\sin(b\cdot\eta) \text{ for Fig 1, } b;$$

$$S(\xi,\eta)=\frac{\xi\cdot e^{j\cdot x_0\cdot\xi}}{\left(\xi^2+\eta^2\right)}\cdot\sin(b\cdot\eta) \text{ for Fig 1, } c;$$

$$\gamma=\sqrt{\xi^2+\eta^2-j\cdot\sigma\cdot\mu_0\cdot\mu_r\cdot\left(\upsilon_x\cdot\xi+\upsilon_y\cdot\eta\right)+j\cdot\omega\cdot\sigma\cdot\mu_0\cdot\mu_r};$$

$$\lambda_0=\frac{\left\{\gamma^2-\mu_r^2\cdot\left(\xi^2+\eta^2\right)\right\}\cdot\left(1-e^{-2\cdot\gamma\cdot d}\right)}{\left(\gamma+\mu_r\cdot\sqrt{\xi^2+\eta^2}\right)^2-\left(\gamma-\mu_r\cdot\sqrt{\xi^2+\eta^2}\right)^2\cdot e^{-2\cdot\gamma\cdot d}};$$

$$\nu_0=\frac{4\cdot\mu_r\cdot\gamma\cdot\sqrt{\xi^2+\eta^2}\cdot e^{\left(\sqrt{\xi^2+\eta^2}-\gamma\right)d}}{\left(\gamma+\mu_r\cdot\sqrt{\xi^2+\eta^2}\right)^2-\left(\gamma-\mu_r\cdot\sqrt{\xi^2+\eta^2}\right)^2\cdot e^{-2\cdot\gamma\cdot d}}.$$

To obtain solution to equation (4) the inverse Fourier transform is applied to the found images (7):

$$B(x,y,z)=\frac{1}{4\cdot\pi^2}\int_{-\infty}^{\infty}\int_{-\infty}^{\infty}b(\xi,\eta,z)\cdot e^{-j(x\xi+y\eta)}\mathrm{d}\xi\mathrm{d}\eta, \quad (8)$$

where ξ, η are the variables of integration.

Solving the differential equation (4) gives components of magnetic induction, B_x, B_y, B_z, in spatial coordinates [14, 15]:

$$B_x=\frac{\mu_0\cdot\mu_r\cdot I}{8\cdot\pi^2}\cdot\int_{-\infty}^{\infty}\int_{-\infty}^{\infty}\frac{\xi}{\eta\cdot\left(1-e^{2\cdot\gamma\cdot d}\right)}\times$$
$$\times\left[\left\{-\left(1+\lambda_0\right)\cdot e^{2\cdot\gamma\cdot d}+\nu_0\cdot e^{\left(\gamma-\sqrt{\xi^2+\eta^2}\right)d}\right\}\cdot e^{\gamma\cdot z}+\right.$$
$$\left.+\left\{1+\lambda_0-\nu_0\cdot e^{\left(\gamma-\sqrt{\xi^2+\eta^2}\right)d}\right\}\cdot e^{-\gamma\cdot z}\right]\times$$
$$\times e^{-z_0\cdot\sqrt{\xi^2+\eta^2}}\cdot S(\xi,\eta)\cdot e^{-j(x\cdot\xi+y\cdot\eta)}\mathrm{d}\xi\mathrm{d}\eta, \quad (9)$$

$$B_y=\frac{\mu_0\cdot\mu_r\cdot I}{8\cdot\pi^2}\cdot\int_{-\infty}^{\infty}\int_{-\infty}^{\infty}\frac{1}{\left(1-e^{2\cdot\gamma\cdot d}\right)}\times$$
$$\times\left[\left\{-\left(1+\lambda_0\right)\cdot e^{2\cdot\gamma\cdot d}+\nu_0\cdot e^{\left(\gamma-\sqrt{\xi^2+\eta^2}\right)d}\right\}\cdot e^{\gamma\cdot z}+\right.$$
$$\left.+\left\{1+\lambda_0-\nu_0\cdot e^{\left(\gamma-\sqrt{\xi^2+\eta^2}\right)d}\right\}\cdot e^{-\gamma\cdot z}\right]\times$$
$$\times e^{-z_0\cdot\sqrt{\xi^2+\eta^2}}\cdot S(\xi,\eta)\cdot e^{-j(x\cdot\xi+y\cdot\eta)}\mathrm{d}\xi\mathrm{d}\eta, \quad (10)$$

$$B_z=j\cdot\frac{\mu_0\cdot\mu_r\cdot I}{8\cdot\pi^2}\cdot\int_{-\infty}^{\infty}\int_{-\infty}^{\infty}\frac{\xi^2+\eta^2}{\eta\cdot\gamma\cdot\left(1-e^{2\cdot\gamma\cdot d}\right)}\times$$
$$\times\left[\left\{-\left(1+\lambda_0\right)\cdot e^{2\cdot\gamma\cdot d}+\nu_0\cdot e^{\left(\gamma-\sqrt{\xi^2+\eta^2}\right)d}\right\}\cdot e^{\gamma\cdot z}-\right.$$
$$\left.-\left\{1+\lambda_0-\nu_0\cdot e^{\left(\gamma-\sqrt{\xi^2+\eta^2}\right)d}\right\}\cdot e^{-\gamma\cdot z}\right]\times$$
$$\times e^{-z_0\cdot\sqrt{\xi^2+\eta^2}}\cdot S(\xi,\eta)\cdot e^{-j(x\cdot\xi+y\cdot\eta)}\mathrm{d}\xi\mathrm{d}\eta. \quad (11)$$

Then, components of the current density in the spatial coordinates, x, y and z, are respectively determined from formulas:

$$J_x=\frac{1}{\mu_0\cdot\mu_r}\cdot\left[\frac{\partial B_z}{\partial y}-\frac{\partial B_y}{\partial z}\right];$$

$$J_y=\frac{1}{\mu_0\cdot\mu_r}\cdot\left[\frac{\partial B_x}{\partial z}-\frac{\partial B_z}{\partial x}\right];$$

$$J_z=\frac{1}{\mu_0\cdot\mu_r}\cdot\left[\frac{\partial B_y}{\partial x}-\frac{\partial B_x}{\partial y}\right]. \quad (12)$$

Formulas (9)–(11) contain improper multiple integrals of the first kind. The truncation method is used to compute improper integrals with infinite intervals of integration. In order to implement it, it is necessary to previously represent them in the form of the sum of three integrals one of which is definite and two are improper unspecified integrals which can be neglected with some accuracy.

In real ECP designs, not one turn (Fig. 1, *a*–*c*) but a coil having N turns (Fig. 1, *d*) is used as an excitation structure. Then, in order to calculate the ECD distribution, it is necessary to supplement the mathematical model (9), (11) with integration of the coil cross-section area. For example, for a circular coil with a rectangular cross-section $l\times w$ (Fig. 1, *d*), the area integration is set by expression:

$$\frac{N}{w\cdot l}\cdot\left\{\int_{-w/2}^{w/2}-j\cdot\frac{2\cdot\pi\cdot(r_m+p)\cdot\eta}{\sqrt{\xi^2+\eta^2}}\cdot J_1\left((r_m+p)\cdot\sqrt{\xi^2+\eta^2}\right)\mathrm{d}p\right\}\times$$
$$\times\left\{\int_{l_m-l/2}^{l_m+l/2}e^{-q\sqrt{\xi^2+\eta^2}}\,\mathrm{d}q\right\}=\frac{N}{w\cdot l}\cdot I_s(r_m,w)\cdot I_E(l_m,l), \quad (13)$$

where $I_s(\ )$, $I_E(\ )$ are the corresponding functional dependences with integral operators; $w=r_2-r_1$; $l=l_2-l_1$ are dimensions of the coil cross-section; $J_1(\ )$ is the Bessel function of the 1st kind of the 1st order; $r_m=\frac{r_1+r_2}{2}$ is the mean radius of the coil; $l_m=\frac{l_1+l_2}{2}$ is the mean height of the coil location relative to the TO.

Hereinafter, the set of equations (9)–(12) will be called the "exact" mathematical model of the surface ECP.

5. Results of studying the computational and time resources for "exact" mathematical ECP models

For further calculations of ECD distribution in the TO, a turn with alternating current I of frequency ω was used in these studies as the structure of ECP excitation. This structure is positioned at a height z_0 above a TO having thickness d with a constant specific electrical conductivity σ and magnetic permeability μ_r (Fig. 1, *a*–c). In this case, the turn can be circular with radius r_0 (Fig. 1, *a*) or as a frame with dimensions $a\times b$ in various positions relative to TO, e. g. a frame parallel (Fig. 1, *b*) or perpendicular (Fig. 1, *c*) to TO.

The ECD distribution for excitation coils (Fig. 1, *a*–*c*) was calculated for the case of variation of only two spatial

coordinates, that is, $J=f(x, y)$ by formulas (9)–(12) of the "exact" mathematical model at initial data given in Table 1.

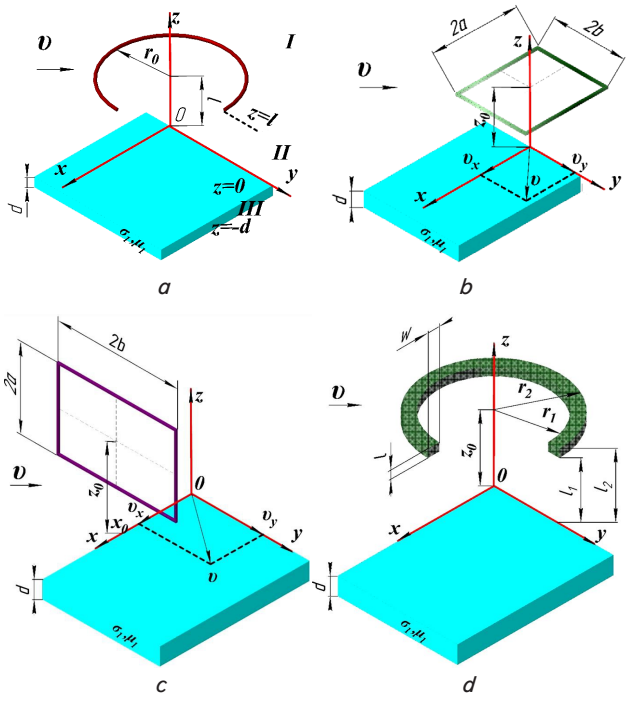

Fig. 1. Geometric model of the ECP excitation coil: a circular turn (*a*); a rectangular turn (frame) (*b*); a rectangular turn (tangential frame) (*c*); a circular coil with rectangular cross-section (*d*)

Numerical results were obtained using the MathCad 15 application package with the following resource support: CPU Intel (R) Core i5 PC, 2.9 GHz, 8 Gb RAM, 64-bit operating system.

Table 2 shows the results of calculation of ECD distribution for the circular excitation coil with different geometric dimensions of the coil r_0 and, respectively, with a stationary TO and taking into account its speed of motion along one component. For a stationary TO, distribution of ECD was symmetrical with respect to the coordinate axes *Ox*, *Oy*, so the number of points for calculation was set only in the quadrant I and equal to 625. For the case of taking into account speed along one component, for example, υ_x, the ECD distribution was symmetric with respect to one coordinate axis, *Ox*, that is, points for calculation were set in quadrants I and II. Their number was 1325.

The timetable for calculating the ECD distribution by the "exact" mathematical model for cases of a stationary probe and taking into account the speed effect was from 3.5 to 20 hours, respectively.

The results of calculation of ECD distribution for the rectangular excitation coil with the same geometric dimensions (40×20 mm) and taking into account the speed of the TO movement along one and two components are given in Table 3.

For a stationary TO, ECD distribution was symmetric with respect to the coordinate axes *Ox, Oy*, so the number of points for calculation was set only for the quadrant I and was 274. For the case taking into account speed along one component, e. g. υ_x, ECD distribution was symmetric with respect to one coordinate axis *Ox*, that is, points for calculation were set in quadrants I and II and their number was 534. When taking into account speed along two components, υ_x, υ_y, the number of points for calculation was 1024 and they were set in quadrants I–IV.

Thus, there were considerable timetables for calculation of the ECD for a rectangular probe: 2.5 to 9 hours, respectively, for cases of stationary ECP and with consideration of the speed effect.

Table 4 shows the results of calculation of ECD distribution for a rectangular excitation coil (tangential ECP) at various geometric dimensions of the coil and with consideration of speed of the TO moving along one or two components as well as for a stationary TO. For the variant of distribution in Table 4 *a–d*, calculation was made at coil dimensions of 12×12 mm and 12×24 mm for the distribution variant in Table 4 *e*–h.

For a stationary TO, distribution of ECD was symmetrical with respect to the coordinate axes *Ox*, *Oy*, so the number of points for calculation was set only for quadrant I and was equal to 576. For the case of taking into account speed of movement in direction of one component, υ_x, distribution of ECD was symmetrical with respect to one coordinate axis, *Ox*, that is, the points for calculation were set in quadrants I and II and their number was 1116. For the υ_y speed component, points were set in quadrants I and IV and their number was 1136; and for the υ_x, υ_y speed components, 2201 points were set in quadrants I–IV.

For this case of the ECP design, timetable for calculation of ECD was also rather large: 2–3 hours for a stationary probe and 4–9 hours with consideration of the speed effect.

To reduce calculation time, it makes sense to substitute a surrogate model, that is, a metamodel, for the "exact" mathematical model. Such a substitution was made, for example, in studies [16, 17] where numerous examples of construction of metamodels of a stationary circular ECP with excitation structures in a form of a single turn of infinitely small cross-section and a coil with rectangular cross-section were illustrated. Calculations using the obtained metamodels indicate a significant reduction in computation time corresponding to 20 and 35 seconds of total time for all points in the testing zone. The comparative analysis convincingly demonstrates the computational efficiency of using metamodels.

Table 1

Initial data for calculating the eddy current density

Geometrical model of the ECP excitation coil	Dimensions of the testing zone, x×y, mm	Height of ECP position above TO z_0, mm	Excitation coil feed current I, A	Alternating current frequency f, Hz	Control object thickness d, mm	Electrophysical parameters of the TO
Fig. 1, *a*	50×50	3	1	100	10	$\sigma = 2{,}5 \cdot 10^6\ S/m$, $\mu_r = 1$
Fig. 1, *b*	80×48	10				
Fig. 1, *c*	15×35	3				

Table 2

Timetable for calculation of the ECD distribution for a circular excitation coil

$\vec{\upsilon}=(\upsilon_x;\upsilon_y), m/s$	Variant of ECD distribution	Σt_{cal}, hr	r_0, mm	ECD distribution
(0; 0)	a	3.5	5	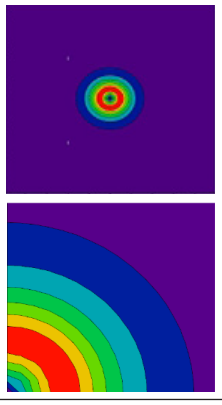
(40; 0)	b	8		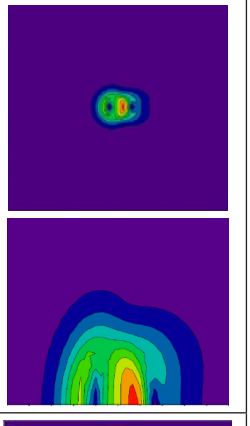
(0; 0)	c	8	25	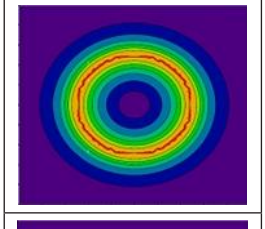
(40; 0)	d	15		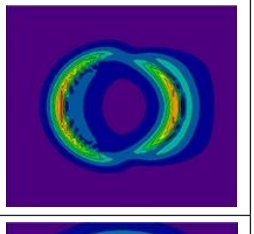
(0; 0)	e	11	35	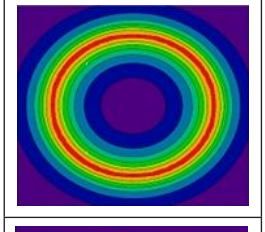
(40; 0)	f	20		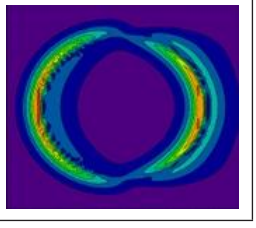

Table 3

Timetable for calculation of the ECD distribution for a rectangular excitation coil

$\vec{\upsilon}=(\upsilon_x;\upsilon_y), m/s$	Variant of ECD distribution	Σt_{cal}, hr	ECD distribution
(0;0)	a	2.5	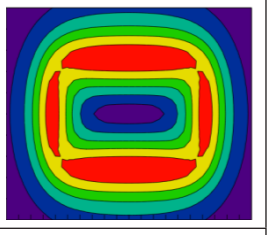
(10;0)	b	3–4	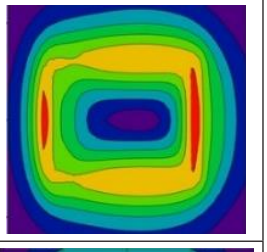
(0;10)	c	3–4	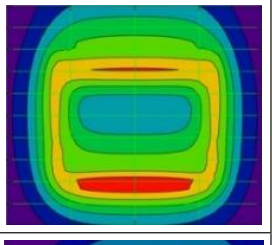
(10;10)	d	7–8	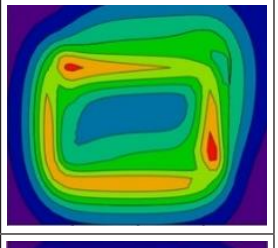
(20;0)	e	5	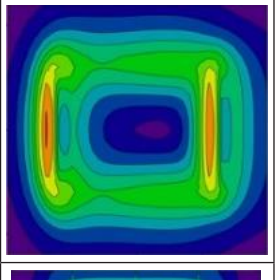
(0;20)	f	5	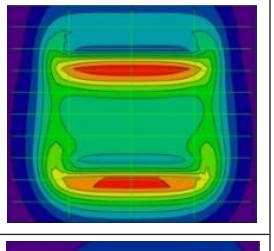
(20;20)	g	8–9	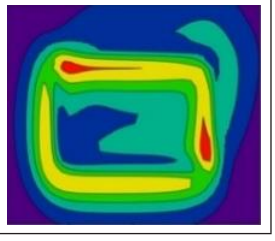

Table 4

Timetable for calculation of ECD distribution for a rectangular coil of excitation of a tangential ECP

$\vec{\upsilon}=(\upsilon_x;\upsilon_y)$, m/s	Variant of ECD distribution	Σt_{cal}, hr	ECD distribution
(0;0)	a	2	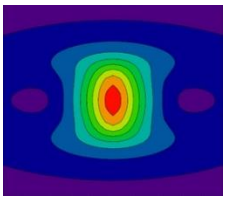
(40;0)	b	4	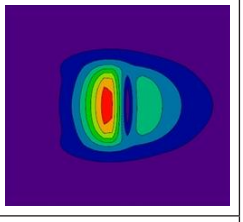
(0;40)	c	4	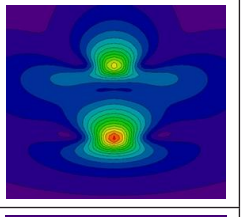
(40;40)	d	7	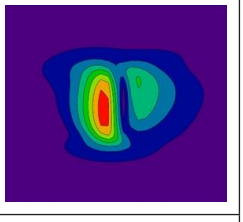
(0;0)	e	3	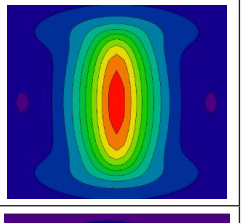
(40;0)	f	5–6	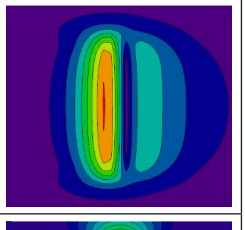
(0;40)	g	5–6	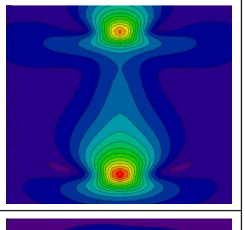
(40;40)	h	8–9	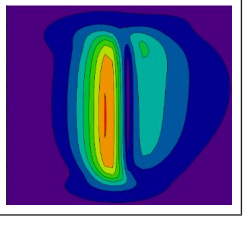

6. Discussion of the results obtained in the study of the resource need for mathematical models

The results obtained in numerical experiments allow us to draw the following conclusions useful in an optimal synthesis of various surface ECP. They also make it possible to suggest solutions to emerging issues.

Data from Table 2 show that the time spent in calculation of ECD distribution for the circular excitation coil at a stationary TO becomes almost three times as large with growth of the coil geometrics. The calculation time does not significantly increase with taking into account the TO speed. For example, comparing the results for identical geometric dimensions of turns, the time taken with an account for one speed component is 23 seconds per point of the testing zone vs. 20 seconds for the stationary TO or 9 hours vs. 7.5 hours for 1325 points.

Analysis of Table 3 shows that the total timetable is not significantly affected by the TO movement speed. For example, calculation time in one point is about 28–33 seconds regardless of the number and nature of the speed components taken into account. Since calculation time depends on the number of calculation points, the increase in the geometric dimensions of the ECP and accordingly the testing zone necessitates an increase in the number of points which automatically make larger the time resource needed for calculation. At the same time, the number of calculation points essentially depends on symmetry of the ECD distribution relative to the coordinate axes.

Table 4 shows the timetable for calculating ECD distribution for a rectangular excitation coil (tangential ECP). As in the previous case, the speed of movement almost does not affect the calculation time which is 12–18 seconds in this case for one point of the testing zone. Also, dependence of time on the increase in geometric dimensions of the coil is observed where it is equally essential for which of the quadrants the calculation is made.

It is clear that calculation time will increase significantly if the optimal synthesis problem is multiparameter, for example, $J=f(x, y, z)$ and solution of the synthesis problem in this case is problematic in general.

This problem is solved by application of the computationally simpler ECP metamodel in the optimization algorithm. That is, to formulate the goal function (1), the ECP metamodel is used which makes it possible to avoid the problem of unlimited growth of computational resource requirements in solving problems of optimal synthesis [16–18].

This study is useful for specialists in non-destructive testing in the field of mechanical engineering. The study results can be used to improve the ECP designs with improved metrological characteristics. Such ECPs feature homogeneous sensitivity, localization of the probing excitation field, improved noise immunity and the ability to get rid of the edge effect manifestations in testing.

The obtained study results can be used as the basis for construction of ECP metamodels for the further surrogate optimal synthesis of various probes with the above properties.

In conclusion, it should be noted that the “exact” mathematical models of surface ECP are costly in the computational sense and cannot be used directly in optimal synthesis as the target function components. The disadvantages of the study include carrying out of numerical experiments just for the case of the ECD dependence on two spatial coordinates. An increase in the number of independent arguments in the function of the ECD calculation which is appropriate for

real synthesis problems will result in even larger computational burden what is unacceptable. The prospect of further development of the study data consists in construction of metamodels for all cases of design of the moving ECP excitation structures.

7. Conclusions

1. Computer models to determine modeling timetable have been constructed on the basis of "exact" electrodynamic mathematical models of surface ECPs.

2. The numerical model experiments have established the following:

– for a circular coil of ECP excitation with dimensions of the testing zone 50×50 mm, ECD distribution calculation time with application of the "exact" mathematical model was 8 to 20 hours taking into account speed υ_x=40 m/s;

– for a rectangular coil of ECP excitation with dimensions of the testing zone 80×48 mm, the ECD distribution calculation time with application of the "exact" mathematical model was 8 to 9 hours taking into consideration speed in direction of two components υ_x, υ_y=20 m/s;

– for a rectangular coil of tangential ECP excitation with dimensions of the testing zone 12×12 mm with dimensions of testing zone 15×35 mm, the ECD distribution calculation time with application of the "exact" mathematical model was more than 7 hours taking into consideration the speed in direction of two components υ_x, υ_y=40 m/s;

– for the testing zone dimensions 12×24 mm, the ECD distribution calculation time was longer than 9 hours at υ_x, υ_y=40 m/s.

3. Estimation of timetable was made and it was found that the "exact" mathematical ECP models cannot be directly used in the problems of optimal synthesis of probes because of substantial computational resource needs, even for a simplified case taking into account two spatial coordinates. Thus, the necessity of using a mathematical apparatus of surrogate optimization with metamodels created on the basis of "exact" electrodynamic models was substantiated for designing moving ECPs with a homogeneous ECD distribution in the testing zone.

References

1. Steblev Yu. I. Sintez vihretokovyh preobrazovateley s zadannoy strukturoy vozbuzhdayushchego polya v zone kontrolya // Defektoskopiya. 1986. Issue 4. P. 58–64.
2. Halchenko V. Ya., Pavlov O. K., Vorobiov M. O. Neliniynyi syntez mahnitnykh poliv zbudzhennia vykhrostrumovykh peretvoriuvachiv defektoskopiv // Metody i prylady kontroliu yakosti. 2002. Issue 8. P. 3–5.
3. Galchenko V. Y., Vorobev M. A. Structural synthesis of attachable eddy-current probes with a given distribution of the probing field in the test zone // Russian Journal of Nondestructive Testing. 2005. Vol. 41, Issue 1. P. 29–33. doi: https://doi.org/10.1007/s11181-005-0124-7
4. Optimization of coil design for eddy current testing of multi-layer structures / Su Z., Ye C., Tamburrino A., Udpa L., Udpa S. // International Journal of Applied Electromagnetics and Mechanics. 2016. Vol. 52, Issue 1-2. P. 315–322. doi: https://doi.org/10.3233/jae-162030
5. Optimization of coil design for near uniform interrogating field generation / Su Z., Efremov A., Safdarnejad M., Tamburrino A., Udpa L., Udpa S. S. // AIP Conference Proceedings. 2015. Vol. 1650. doi: https://doi.org/10.1063/1.4914636
6. Stawicki K., Gratkowski S. Optimization of Exciter Coils in Eddy Current Transducer for Testing Thick Conducting Plates // Electromagnetic Fields in Mechatronics Electrical and Electronic Engineering. Proceedings of ISEF'05. 2006. P. 497–502.
7. Janoušek L. Effect of exciting system configuration on eddy currents distribution in non-destructive evaluation of materials // Przegląd elektrotechniczny. 2013. Vol. 89, Issue 3a. P. 256–258.
8. Ye C., Udpa L., Udpa S. Optimization and Validation of Rotating Current Excitation with GMR Array Sensors for Riveted Structures Inspection // Sensors. 2016. Vol. 16, Issue 9. P. 1512. doi: https://doi.org/10.3390/s16091512
9. Visualization of Eddy Current Distributions for Arbitrarily Shaped Coils Parallel to a Moving Conductor Slab / Itaya T., Ishida K., Kubota Y., Tanaka A., Takehira N. // Progress In Electromagnetics Research M. 2016. Vol. 47. P. 1–12. doi: https://doi.org/10.2528/pierm16011204
10. Magnetic Field Analysis of an Arbitrary Shaped Coil Using Shape Functions / Ishida K., Itaya T., Tanaka A., Takehira N. // IEEE Transactions on Magnetics. 2009. Vol. 45, Issue 1. P. 104–112. doi: https://doi.org/10.1109/tmag.2008.2005119
11. Panas S., Kriezis E. E. Eddy current distribution due to a rectangular current frame moving above a conducting slab // Archiv für Elektrotechnik. 1986. Vol. 69, Issue 3. P. 185–191. doi: https://doi.org/10.1007/bf01574623
12. Numerical and experimental study of eddy current probes in NDT of structures with deep flaws / Thollon F., Lebrun B., Burais N., Jayet Y. // NDT & E International. 1995. Vol. 28, Issue 2. P. 97–102. doi: https://doi.org/10.1016/0963-8695(94)00010-h
13. Theodoulidis T., Bowler J. R. Interaction of an eddy-current coil with a right-angled conductive wedge // IEEE Transactions on Magnetics. 2010. Vol. 46, Issue 4. P. 1034–1042.
14. A New Analytical Method for Calculation of the Eddy Current Distribution and its Application to a System of Conductor-Stab and Rectangular Coil / Itaya T., Ishida K., Tanaka A., Takehira N., Miki T. // PIERS Online. 2011. Vol. 7, Issue 8. P. 766–770.
15. Eddy Current Distribution for a Rectangular Coil Arranged Parallel to a Moving Conductor Stab / Itaya T., Ishida K., Tanaka A., Takehira N., Miki T. // IET Science, Measurement & Technology. 2012. Vol. 6, Issue 2. P. 43–51.
16. Trembovetska R. V., Halchenko V. Ya., Tychkov V. V. Metamodeliuvannia yak metod proektuvannia vykhrostrumovykh peretvoriuvachiv z apriori vyznachenymy vlastyvostiamy // Vymiriuvalna ta obchysliuvalna tekhnika v tekhnolohichnykh protsesakh: Materialy XVIII mizhnarodnoi naukovo-tekhnichnoi konferentsiyi. Odessa, 2018. P. 105–107.
17. Halchenko V. Ya., Trembovetska R. V., Tychkov V. V. Neiromerezheva metamodel tsylindrychnoho nakladnoho vykhrostrumovoho peretvoriuvacha yak skladova surohatnoho optymalnoho syntezu // Visnyk Khersonskoho natsionalnoho tekhnichnoho universytetu. 2018. Vol. 1, Issue 3 (66). P. 32–38.
18. Halchenko V. Ya., Trembovetska R. V., Tychkov V. V. Zastosuvannia metamodelei dlia vyrishennia zadach syntezu vykhrostrumovykh peretvoriuvachiv z odnoridnym rozpodilom shchilnosti strumu v zoni kontroliu // Pryladobuduvannia: stan i perspektyvy: materialy XVII Mizhnarodnoi naukovo-praktychnoi konferentsiyi. Kyiv: PBF, NTUU "KPI", 2018. P. 146–147.